

Laboratoire "Transformations
Intégrées de la matière
Renouvelable (TIMIR)
Interfaces et milieux divisés (IMiD)
Université de Technologie
Compiègne, France.

Escola tècnica superior
d'Enginyeria Industrial de Barcelona.
Universitat Politècnica de Catalunya.

FUNCTIONALIZATION OF SILICON CARBIDE BY MAGNETIC NANOPARTICLES FOR TRACER USES

PARRA CARMONA, Alejandro.

PROFESSOR:

BENALI, Mohamed

GUÉNIN, Erwann

Professor Tutor:

SALEH, Khashayar.

July 2017.

Abstract

The present work reports a novel and simple way to functionalize commercial silicon carbide with magnetic nanoparticles (Fe_3O_4). Maghemite and magnetite nanoparticles were synthesized by chemical coprecipitation of $\text{FeCl}_3 \cdot 6\text{H}_2\text{O}$ and $\text{FeCl}_2 \cdot 4\text{H}_2\text{O}$ with a proportion 2:1. This method was selected for its simplicity, reproducibility and low cost in terms of solvents and chemical reagents. They were characterized by transmission electron microscopy (TEM), X-ray diffraction (XRD), magnetometry (MIAtek®) and ultraviolet-visible spectroscopy (UV). The main objective of this work is to study the coating of SiC with Fe_3O_4 in four different situations: synthesis or addition of magnetic nanoparticles, evaporation of water, and use of a binder. The particles were characterized by scanning electron microscopy (SEM), magnetometry (MIAtek®) and Fourier transform infrared spectroscopy (FT-IR). As observed by MIAtek® there is a difference between the methods used, evaporation of water being the best technique to obtain functionalized SiC with 0,5 wt% coated nanoparticles and showing no apparent change on morphology and a high magnetic saturation reachable at low applied field and room temperature, making this method, suitable for tracer uses.

Key words: Nanoparticles – Magnetism – SiC – Functionalization – Fe_3O_4

1. Introduction

Fluidization it is an event adopted in numerous process in engineering with many years of experience. Its first appearance was in 1940, used in the process of catalytic cracking. Since then, there has been multiples studies to understand the procedure and enhance its performance [1]. To figure out fluidized bed compartments, there has been multiples methods, such as bed pressure drop, bubbles rate of ascent, void fraction and pressure variations during the process [2].

Nowadays there are sophisticated methods involving capacitive probes, gamma-ray detectors in-line particle size analyzers, positron emission particle tracking, ultraviolet camera, among others [3][4][5].

High pressure/temperature fluidized beds are large used in chemical industries such as gasification, catalytic cracking, combustion chambers. It is important to understand particles motion inside the reactor. However, there are not many possible methods involving particles movement at such high temperature. Capacitive probes has proven to be a reliable technique to detect it [6].

The particle designed to pass through the sensor will be Silicon carbide (SiC) coated with iron oxide (Fe_3O_4) magnetic nanoparticles. This tracer will maintain SiC properties, making it suitable to use it as a tracer.

SiC is a semiconductor material which improves the performance of Silicon (Si) in microelectronic applications at high temperatures, high power and irradiated systems. SiC particles are used as a heat transfer medium in fluidized beds, in order to collect solar energy radiation in solar thermal plants [6][7]. The improvements of SiC in this process are high heat capacity, good availability and low cost. This promising properties makes

the SiC a suitable candidate in process involving fluidized beds, such as gasification or combustion [5]. The SiC particles used for this experimental work are Saint Gobain, SIKA® ABR IV A F220 with an average particle size ($d_{3,2}$) of 60 μm and density of 3210 k/m^3 .

Regarding the magnetic coating, the objective of this work is to synthesis magnetic nanoparticles (MNP). MNP have applications in several areas such as biomedical [8] or green chemistry [9]. The magnetite, iron oxide paramagnetic, can be produced by different methods including thermal decomposition of organometallic precursors [10], chemical co-precipitation [11][12] or ultrasound irradiation [13]. In this work, Fe_3O_4 were manufactured with co-precipitation method. This method was selected for its simplicity, reproducibility and low cost in terms of solvents and chemical reagents. In this method, Fe^{2+} and Fe^{3+} are generally precipitated in alkaline solutions, sodium hydroxide (NaOH) at 35°C. The size of nanoparticles generated will have a strong impact on their magnetic properties [12].

This experimental work defines and discuss different methods, using liquid precipitation of Fe_3O_4 , to cover SiC particles. Process such as synthesis or addition of MNP, evaporation of water, and use of a binder will be evaluated. The resulting SiC particles are slightly covered with Fe_3O_4 nanoparticles leading to a particle with similar shape and density, making it suitable for tracer uses.

2. Experimental

2.1. Materials and methods

The chemical reagents used to produce MNP (Fe_3O_4) in this work were ferrous chloride tetrahydrate ($\text{FeCl}_2 \cdot 4\text{H}_2\text{O}$), ferric chloride hexahydrate ($\text{FeCl}_3 \cdot 6\text{H}_2\text{O}$), sodium hydroxide

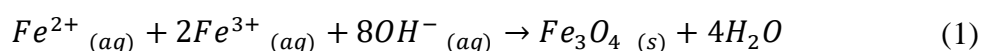
(NaOH) and hydrochloric acid 37% (HCl). All chemicals compounds were of analytical degree. The coating process required silicon carbide (SiC) SIKA® ABR IV A F220, sodium hydroxide (NaOH) and (hydroxypropyl)methyl cellulose (HPMC). Potassium thiocyanate (KSCN), Nitric acid (HNO₃) and Hydrogen peroxide (H₂O₂) were used in the characterization of nanoparticles concentration.

Nanoparticles were synthesized according to the method of alkaline co-precipitation of iron salts in aqueous solutions [11][12]. SiC coating was realized by liquid deposition.

2.2. Synthesis of Magnetite

Three samples of magnetite nanoparticles were prepared by alkaline co-precipitation. A mixing of iron ions in form of hydrated chloride salts were poured in alkaline medium, in the proportion of Fe³⁺/Fe²⁺ of 2/1. Initially, 0,01 mol of FeCl₂·4H₂O were dissolved in 7,5 mL of HCl 1 mol·L⁻¹ to prevent premature oxidation of Fe²⁺ to Fe³⁺ in aqueous solutions. 0.02 mol of FeCl₃·6H₂O were dissolved in 160 mL of water, and mixed with the ferrous solution through an ultrasound bath. Afterwards, the binary solution of Fe²⁺ and Fe³⁺ was added, with a burette of 100 mL, into a solution of NaOH 2 mol·L⁻¹ (84 mL). The addition speed will define nanoparticle size [11]. For 2 h, under constant stirring at 2000 rpm, the solution reacted at constant temperature (35°C).

It is important to note that, when NaOH was used, the binary solution of Fe²⁺ and Fe³⁺ was added over the base contained. The resulting black precipitate was isolated by a magnetic field and washed several times with distilled water, reaching a value of pH equal to 7. This process is characterized by the following chemical equation:



2.3. SiC functionalization with magnetite nanoparticles

Four procedures were prepared for SiC functionalization: synthesis or addition of MNP, evaporation of water, and use of a binder. All of them were carried at basic pH (pH>12), with the same proportion magnetite nanoparticles /SiC (10 wt%).

Procedure 1. The synthesis of magnetite nanoparticles was performed as described in section 2.2. SiC particles were previously weighed and introduced inside the reactor with a quantity of base (NaOH). The binary solution of Fe²⁺ and Fe³⁺ was poured inside the reactor and agitated for 2 h with vigorous stirring at 35 °C. The sample was filtrated and rinsed with abundant water, then dried at 70 °C for 24 h.

Procedure 2. The addition of magnetite nanoparticles was done in the same reactor as procedure 1. SiC particles, previously weighed, were introduced inside the reactor with a quantity of base. This quantity depends on the volume of magnetite nanoparticles used (20 mL NaOH 2 mol·L⁻¹ for 100 mL of MNP). Stable nanoparticles were poured inside the reactor and agitated with vigorous stirring at 35°C. The sample was filtrated and rinsed with abundant water, then dried at 70 °C for 24 h.

Procedure 3. The water evaporation was a similar method as procedure 2. In this case, a Rotavap® was used to evaporate the solvent. The SiC was placed inside the flask with an amount of base and magnetite nanoparticles. The flask was rotated energetically at 50 °C and with a pressure of 75 mbar, until the solvent had been evaporated. Then, the solid was removed from the flask with deionized water, filtrated and washed. At the end, the sample was dried at 70 °C for 24 h.

Procedure 4. The binder (HPMC) was used in procedures 1 (Procedure 4.1) and 3 (Procedure 4.3). In procedure 1, 30 min after pouring the binary solution, the binder was added at a 0,5 wt% of SiC in liquid state. In procedure 3, the binder was added with the

other reagents from the start. To liquefy HPMC, the powder was dissolved in 20 mL of water, then stirred with a magnetic agitator for 20 min at 50 °C.

2.4. Sample Characterization

2.4.1. Transmission Electron Microscope (TEM)

The homogeneity and dimension of nanoparticles test was performed by TEM. The equipment used was a Philips CM10 integrating a head of lanthanum hexaboride (LaB_6) operated at 100 kV. A drop of well dispersed MNP was placed on a copper grid of 2 mm diameter coated with an amorphous carbon film. The solution was dried at room temperature before it was attached to the microscope sample holder.

2.4.2. X-Ray Diffraction (XRD)

The crystallographic analysis of the samples was performed by XRD powder method. Diffraction patterns (2θ) were recorded with a BRUKER D8 ADVANCE diffractometer, equipped with copper cathode ($\text{Cu K}\alpha_1$ 1,54178 Å) and Ni filter, operating at 40 kV and a current of 40 mA. A continuous scan with a step of 0,020 (1 deg/50 s) was used to collect 2θ from 10 to 80 degrees, using DIFRACT.EVA V4.2.1 software to treat the results.

2.4.3. Ultraviolet-Visible Spectroscopy (UV)

The concentration of magnetite nanoparticles was measured by UV method and was carried out in a VWR® UV-6300PC. This equipment has a double beam with deuterium and tungsten lamps, with a wavelength range (nm) 190-1100. There were two analysis done: direct measure on nanoparticles sample and KSCN method (both explained in Concentration determination by the method KSCN). The wave length was 480 nm and 475 nm respectively.

2.4.4. Dynamic light scattering (DLS)

The size distribution profile of nanoparticles was determined by Dynamic light scattering (DLS). The equipment used to determine the distribution was a Malvern model Nano-ZS ZEN 3600. It has a He-Ne laser with 10mW power, lenses, mirrors and attenuators, avalanche photodiode and a numeric correlator.

2.4.5. Scanning Electron Microscope (SEM)

The SiC morphology was examined by scanning electron microscopy (SEM). The equipment used was a FEI Quanta 250 FEG, operated at 20 kV and using a lens amplification between 100 and 400.

2.4.6. Fourier transform infrared spectroscopy (FT-IR) and Attenuated Total Reflection (FTIR-ATR)

FT-IR was used to detect the characteristic bands for Fe-O and complement the information of XRD method on the magnetite nanoparticles samples. The equipment used from Thermo Scientific is a Nicolet 380. It has a Globar lamp with a SiC stick, emitting from 250 to 10000 cm^{-1} , a separator (Germanium and potassium bromide KBr), interferometer and a pyroelectric detector (DRGS type). The data has been treated with OMNIC software. The Fe-O characteristic bands inside Fe_3O_4 nanoparticles were 452 and 585 cm^{-1} [14][15]. Attenuated total reflexion (ATR) installed on a Nicolet 6700 was used, in the middle infrared region (3850-675 cm^{-1}), to study SiC samples to detect Fe_3O_4 coating.

FT-IR (KBr): 452 cm^{-1} , 585 cm^{-1} , 632 cm^{-1} , 1384 cm^{-1} , 1618 cm^{-1} 3384 cm^{-1} .

2.4.7. Magnetic Properties

Magnetic properties of the samples were tested in the MIAtek® equipment. MIAtek® allows to measure the third derivative for the magnetic induction in relation with the excitation field $S_3(H) = \partial^3 B(H) / \partial^3 H$ (MIAtek® units) where the field H is null. An alternative double excitation field is applied with a low frequency (LF) and high amplitude ($f_0 = 0,025$ Hz and $A_0 = \pm 36$ kA·m⁻¹) and a field with high frequency (HF) and low amplitude ($f_1 = 24,4$ kHz and $A_1 = \pm 0,707$ kA·m⁻¹). This equipment measures the harmonic tension related to the frequency $f_1 - 2f_0$, being the tension, proportional to the concentration of superparamagnetic nanoparticles in the sample.

3. Results and Discussion

3.1. Magnetite Nanoparticles

One of the main objectives of this work was to produce magnetite nanoparticles, in order to obtain SiC functionalized. To do so, MNP should be small enough to coat the surface of SiC, and sufficiently large to obtain a suitable magnetism. To do so, MNP were produced with co-precipitation method, using NaOH, the base. The characterization of iron oxide was obtained by XRD and FT-IR analysis. Size distributions of MNP synthesized in this work were obtained by analysis of TEM images and Zetasizer® analysis.

The crystallization of the iron oxide was characterized by XRD, shown on Figure 3.1. The pattern of X-ray diffraction corresponds to samples of magnetite with copper cathode shown in *Mascolo* [12]. Near the most intense peak, at 35,2° (2θ), there is a band corresponding to salt. This salt, originates in the nanoparticles cleaning. It is due the use of acid and base to adjust to a pH 7.

Although the bands are characteristic for magnetite (Fe_3O_4), they also concur with maghemite. The sample had a black perception indicating more concentration of Magnetite than Maghemite. To assure the composition of Fe_3O_4 , a FT-IR was realized, shown on Figure 3.2. The presence of magnetite can be confirmed by the three absorption bands at 452, 585 and 632 cm^{-1} . The spectrum prove the characteristic strong absorption band at 585 cm^{-1} , which comes from the Fe-O typical vibration of magnetite [15].

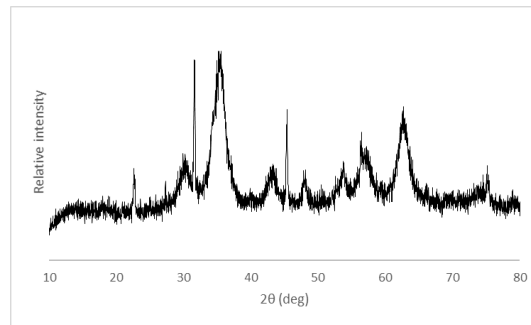


Figure 3.1. X-ray diffraction (XRD) patterns with copper radiation of MNP obtained with co-precipitation method

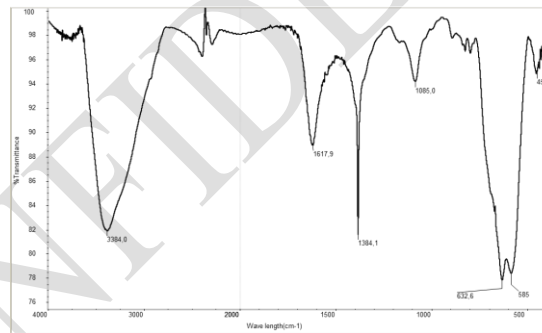


Figure 3.2. FT-IR image for MNP prepared by co-precipitation method.

Once the most intense peak was determined at $35,2^\circ$ (2θ), Scherrer's equation (equation 4) was used to calculate the average nanoparticle diameter [16]:

$$D_{(hkl)} = \frac{K \cdot \lambda}{b_{(hkl)} \cdot \cos \theta} \quad (2)$$

The equation uses the reference peak width at angle θ , analogous to Bragg's angle, where λ is the X-Ray wavelength (Cu $K\alpha_1$ 1,54178 \AA), b is the width of the XRD peak ($35,2^\circ$

(2θ)) at half height, and K is a shape factor of approximately 0,93 for magnetite and maghemite[16]:

$$K = 2 \cdot \left(\ln\left(\frac{2}{\pi}\right)\right)^{1/2} = 0,93 \quad (2)$$

Once used the Scherrer's formula, an estimation can be done regarding the dimension of the crystalline diameter of nanoparticles. In this case the diameter was approximately 6,3 nm.

This can be corroborated with the TEM study and DLS studies. TEM study, shown in Figure 3.3, presents nanoparticles distribution with some agglomerations. The size of the nanoparticles it is less than 10 nm, approaching the crystalline diameter shown in XRD study. The agglomerations can be demonstrated on the DLS study, were appears a peak with a wide range, present in Figure 3.4. Nanoparticles synthetized had a hydraulic diameter (in number) of $17,8 \pm 6,42$ nm with a polydispersity of 0,41. This polydispersity of 0,41 proves the agglomerations within the standard limits for DLS analysis regarding co-precipitation methods (shown in ISO 22412:2017)

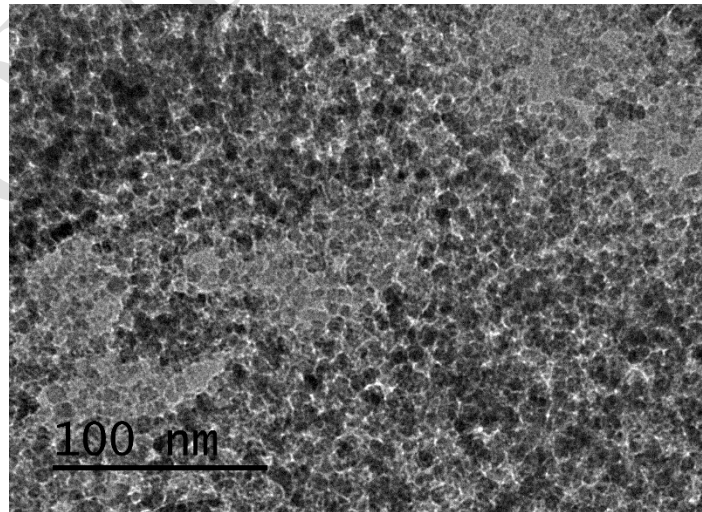


Figure 3.3. TEM image of magnetite nanoparticles prepared by co-precipitation method. Scale bar: [100 nm]

The Zeta potential, $26,8 \pm 7,35$ mV shows a positive potential on the surface of the nanoparticles. If the Zeta potential tends to zero, there is going to be more clusters in the sample. The sign of the Zeta potential is explained in the way nanoparticles are preserved. Those nanoparticles are stored at $\text{pH} = 2$. This indicates, on the surface of nanoparticles, there is a layer of H_3O^+ . This positive charge, repulse the other nanoparticles to avoid the formation of clusters. The possible explanation for agglomeration in this case is, although there is a positive charge on the nanoparticles surface, the size is small enough to overcome the electric charge. Thereby, their internal energy (Van der Waals attraction force) is large enough to overcome the electrical repulsion from the MNP [12][17].

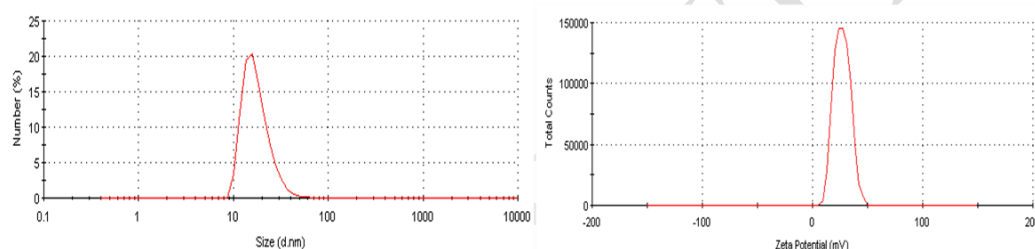


Figure 3.4. Zetasizer analysis of MNP with size distribution and zeta potential

The results on magnetic performance were displayed by MIAtek[®] analysis. Table 3.1 indicates the relation between Miatek[®] results and crystalline diameter. The nanoparticles synthesized had a crystalline diameter of $6,05 \pm 0,94$ nm. As it can be seen, the magnetism on the different samples increases with the crystalline diameter. This increase rate has been corroborated in numerous publications and can be related with the inter-particle interaction, which depends on particle size, inter-particle spacing and the presence of a spin disorder layer on nanoparticles surface [18].

MIA/mg Fe ₃ O ₄	Crystalline diameter (nm)
262948	6,8
81983	6,34
77593	5

Table 3.1. Relation between MIAtek[®] results and crystalline diameter

3.2. SiC functionalization with Fe₃O₄ nanoparticles

Figure 3.5 presents the results of SiC functionalized with MNP. In this picture, there is no substantial difference between methods. SiC used for this experiments, SIKA® ABR IV A F220 with an average particle size ($d_{3,2}$) of 60 μm and density of 3210 kg/m^3 , it is a particle with a plane surface without noticeable pores. SEM corroborates it. Magnetite nanoparticles (white dot) can be found in the irregularities of SiC particles surface and tends to concentrate on defects on the surface. Traces of Vanadium (V) and Titanium (Ti) were found on the SiC elemental analysis. Those elements tend to create irregularities on the exterior of SiC, improving the deposition of Fe₃O₄ nanoparticles.



Figure 3.5. Surface SEM images of the SiC coated with Fe₃O₄ nanoparticles: (a) SiC blank; (b) Procedure 1; (c) Procedure 2; (d) Procedure 3; (e) Procedure 4.1; (f) Procedure 4.3

From the elemental analysis for the SiC samples (Figure 3.6), a percentage of Fe can be identified. This value can only be used to acknowledge the process of nanoparticles deposition (detect iron nanoparticles on SiC surface) but it cannot be used as a quantifier, because it depends on the sample placed inside the SEM. The following results came back (on % Fe): (b) 1,64; (c) 2,90; (d) 1,87; (e) 3,38; (f) 0,08. All of them had the same magnitude, except sample (f). The procedure 4.3, which involves binder and Rotavap,

had issues regarding solvent evaporation. Bubbles were formed on the liquid-solid surface during the experiment. This might be the reason for this 0,08% of iron, the lack of magnetite nanoparticles deposition on SiC surface.

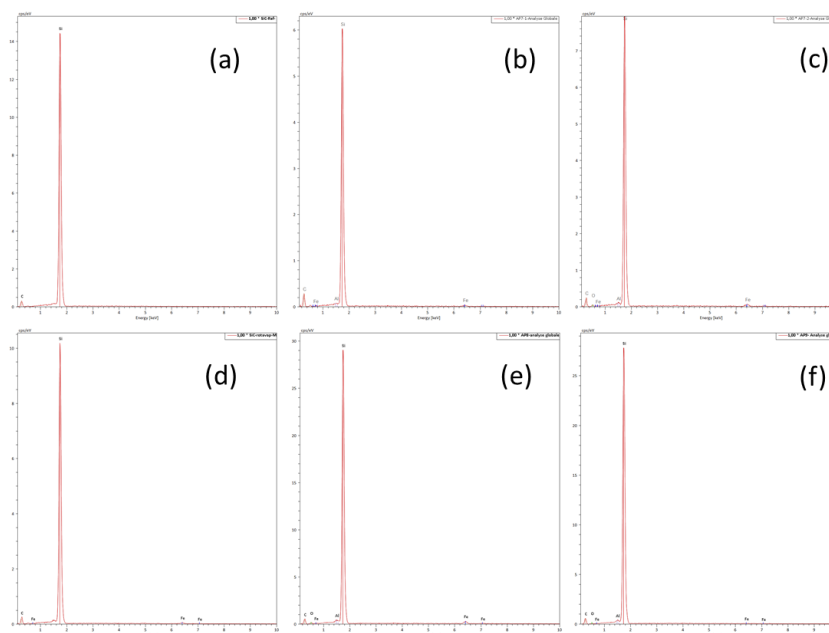


Figure 3.6. Elemental analyses of the SiC coated with Fe_3O_4 nanoparticles: (a) SiC blank; (b) Procedure 1; (c) Procedure 2; (d) Procedure 3; (e) Procedure 4.1; (f) Procedure 4.3

On the following image, Figure 3.7, FTIR-ATR image was made to detect surface coating. Si- band appears between 1000 and 1500 cm^{-1} and Si-C bond appears between 850 cm^{-1} [19][20]. As it can be seen in Figure 3.7, 3 bands, at approximately 1200 cm^{-1} , 1000 and 850 cm^{-1} on the SiC Coated decreases. This drops indicates a change on SiC surface. In this case, SiC characteristic bands have been covered with Fe_3O_4 nanoparticles.

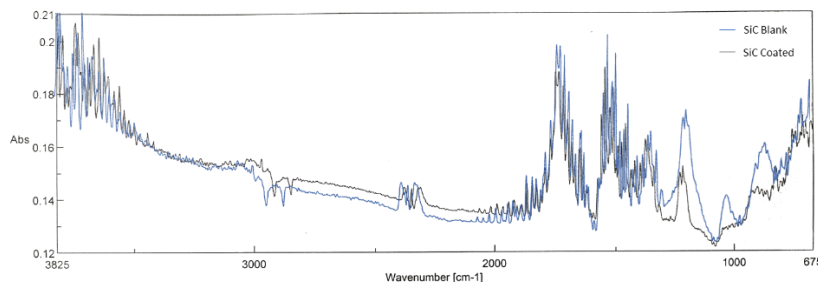


Figure 3.7. FTIR-ATR SiC Blank and SiC Coated

The same procedures have been tested on Silica (SiO_2). SiO_2 is the opposite of SiC with nano-pores on its surface. It was acquired from MP EcoChrom™ with an average particle size ($d_{3,2}$) of 63-200 nm with active nano-pores of 6 nm. Figure 3.8 display the different SiO_2 coated with Fe_3O_4 .

The experiments conducted on SiO_2 were procedure 2 and procedure 3. As it can be seen on Figure 3.8 procedure 2 has changed SiO_2 morphology, breaking up Silica particles, through mechanical agitation. The change on the surfaces triggered a major deposition of MNP (more white dots on the surface). Procedure 3 produced homogeneous dispersion along the sample, creating better results, in terms of dispersion, than with SiC. This is corroborated on the elemental analysis where iron peaks were far more intense than with SiC. The results on percentage of iron (% Fe) were: (b) 14,65;(c) 9,92. There is an increment over 700% over SiC experiments.

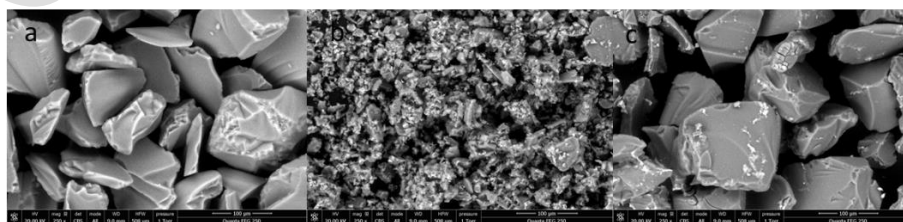


Figure 3.8. Surface SEM images of the SiO_2 coated with Fe_3O_4 nanoparticles: (a) SiO_2 blank; (b) Procedure 2; (c) Procedure 3

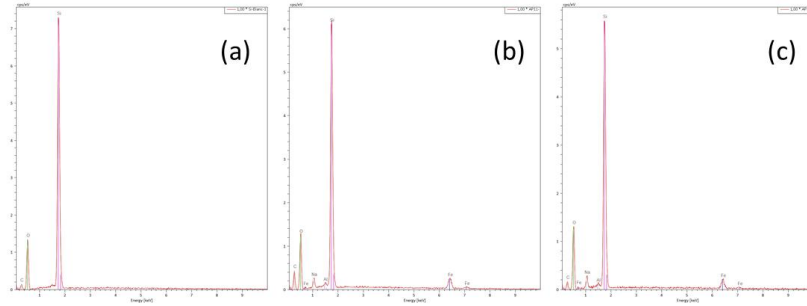


Figure 3.9. Elemental analyses of the SiO_2 coated with Fe_3O_4 nanoparticles: (a) SiO_2 blank; (b) Procedure 2; (c) Procedure 3

On Table 3.2 results on magnetism are shown. The procedures with a higher grade of magnetism are procedure 2 and 3, being procedure 3 the best way to achieve an acceptable level of magnetism. The percentage of iron was calculated through MIAtek® results on Fe_3O_4 nanoparticles display on Table 3.1. Due to the inability to recuperate the ferrofluid on procedure 1, there are no MIAtek® studies on such nanoparticles, therefore no results on the percentage of iron nanoparticles.

$$\% \text{MNP} = \frac{(\text{MIAtek mag. SiC} - \text{MIAtek SiC Blank}) \times \text{MNP weight}}{\text{MIAtek MNP} \times \text{Mag. SiC weight}} \times 100 \quad (2)$$

The procedures with the lowest magnetic performance were procedure 4, because of binder usage. Binder can suppress the deposition of nanoparticles on SiC surface, granulating the Fe_3O_4 into larger units, being unable to coat SiC surface. Another possibility could be that HPMC (binder) is unable to cover SiC due to its large surface. Nanoparticles are formed through the nucleation and growth of superparamagnetic primary particles [18]. The variation on concentration, solutions homogeneity, pH, temperature can affect the formation of those nucleation. In procedure 1, the introduction of SiC can

affect the mixing homogeneity, impacting on the formation of nanoparticles. This could be an explanation of the poor results in MIAtek® study.

	Procedure	MIA/g substrate	w% Fe ₃ O ₄
SiC	1	250235	NR
	2	720576	0,28
	3	1311090	0,5
	4.1	29980	NR
	4.3	199829	0,25
SiO ₂	2	3720000	4,82
	3	939129	1,23

Table 3.2. Results on magnetism for SiC coating with percentage of Fe₃O₄ nanoparticles on SiC/SiO₂ surface. [NR]: No Results

The comparison between SiC and SiO₂ coating was done by procedure 2 and 3, with the procedure 3 as the best performance in MIAtek® results. As it can be seen in Table 3.2 the percentage of Fe₃O₄ nanoparticles corroborates the results realized with SEM (Figure 3.6 and Figure 3.9), where percentage of Fe₃O₄ on Silica duplicates the quantity on SiC. This is mainly caused by the nano-pores on SiO₂ allowing the intensification on MNP deposition. However, in this case, the increase on percentage of Fe₃O₄ percentage does not imply an increase on MIAtek® measures. MIAtek® gives a higher signal if nanoparticles are aggregated. In SiO₂, the homogeneity on its surface regarding Fe₃O₄ deposition could be decreasing MIAtek® readings. If there is a major dispersion with low agglomerates, MIAtek® measures will drop. As *Mascolo* said in his study: “Magnetics values decrease as the magnetite particle size decreases” [12].

4. Conclusion

A cheap co-precipitation and mixing method has been utilized to synthesize magnetite nanoparticles and functionalize SiC particles. As observed by TEM and DLS, the nanoparticles synthesized with a standard polydispersity for a co-precipitation method, with a crystalline diameter of 6 nm and a D_H of 17,8 nm. From XRD pattern and FT-IR

analysis, it appears that the obtained nanoparticles correspond to magnetite and maghemite, with high magnetization saturation reachable at low applied field and superparamagnetic behavior at room temperature.

Results from SEM and MIAtek® display the better method to functionalize SiC as procedure 3, showing no apparent change on morphology and a high magnetic saturation reachable at low applied field. Making these particles, suitable for tracer uses.

5. Further steps

In this work, it has been demonstrated that SiC can be functionalized with MNP with low cost and being environmental friendly. To enhance SiC functionalization, an increment on MNP diameter will increase its magnetism. In order to corroborate the utilization of magnetic SiC as a tracer, a granulometry study should be carried out to confirm there has not been any modifications on SiC morphology. Then, the next step will be the detection and separation method in a fluidized bed. First, creating a probe with a high detection rate and then a separation method will be investigated, in order to capture all MNP.

Nowadays, fluorescent cameras had been developed and studied [21], to detect particle motion and dispersion patterns. A good solution to use those cameras, will be to develop SiC particle with double function: Magnetic and Fluorescent. The fluorescent nanoparticles designed for SiC coating will be zinc sulfide (ZnS) [22]–[25]. With this dual function, it can be used on other types of particles such a silica.

6. Acknowledgements

This work was supported by university of technology of Compiègne, dept. TIMIR and IMiD. I want to personally thank Benali, Mohammed and Guénin, Erwann for their support during this work, and Khashayar, Saleh for the confidence placed in me.

CONFIDENTIAL

7. Bibliography

- [1] S. C. Shamkuwar, D. N. Malkhede, and S. Ugile, “ScienceDirect Critical Study on Rotary Fluidized bed as a Diesel Particulate Filter using SiC particles,” *Mater. Today Proc.*, vol. 4, no. 2, pp. 653–659, 2017.
- [2] B. Moreno and V. Manuel, “Estudio hidrodinámico de un lecho fluidizado,” 2007.
- [3] B. Hage and J. Werther, “POWDER TECHNOLOGY The guarded capacitance probe a tool for the measurement of solids flow patterns in laboratory and industrial fluidized bed combustors,” vol. c, no. 97, pp. 235–245, 1997.
- [4] V. Wiesendorf and J. Werther, “Capacitance probes for solids volume concentration and velocity measurements in industrial fluidized bed reactors,” vol. c, 2000.
- [5] D. Valdesueiro, P. Garcia-triñanes, G. M. H. Meesters, M. T. Kreutzer, and J. Gargiuli, “Nuclear Instruments and Methods in Physics Research A Enhancing the activation of silicon carbide tracer particles for PEPT applications using gas-phase deposition of alumina at room temperature and atmospheric pressure,” vol. 807, pp. 108–113, 2016.
- [6] C. Tregambi, R. Chirone, F. Montagnaro, P. Salatino, and R. Solimene, “ScienceDirect Heat transfer in directly irradiated fluidized beds,” *Sol. Energy*, vol. 129, pp. 85–100, 2016.
- [7] G. Flamant, D. Gauthier, H. Benoit, J. Sans, R. Garcia, B. Boissière, R. Ansart, and M. Hemati, “Dense suspension of solid particles as a new heat transfer fluid for concentrated solar thermal plants : On-sun proof of concept,” *Chem. Eng. Sci.*, vol. 102, pp. 567–576, 2013.
- [8] R. Müller, M. Zhou, T. Liebert, J. Landers, S. Salamon, S. Webers, A. Dellith, D. Borin, T. Heinze, and H. Wende, “Mobility investigations of magnetic nanoparticles in biocomposites,” *Mater. Chem. Phys.*, vol. 193, pp. 364–370, 2017.
- [9] R. Starbird-Pérez and V. Montero-Campo, “Síntesis de nanopartículas magnéticas de óxido de hierro para la remoción de arsénico del agua de consumo humano,” *Tecnol. en Marcha*, vol. 28, no. 3, pp. 45–54, 2015.
- [10] P. Nguyen, “Patrick Nguyen Optimisation of the β -SiC based catalyst for the selective oxidation of H₂S into elemental sulphur , from the laboratory to industry .,” 2006.
- [11] R. MASSART and V. CABUIL, “SYNTHÈSE EN MILIEU ALCALIN DE MAGNETITE COLLOÏDALE: CONTRÔLE DU RENDEMENT ET DE LA TAILLE DES PARTICULES,” vol. 5, no. 11, pp. 2–8, 1987.
- [12] M. C. Mascolo, Y. Pei, and T. A. Ring, “Room Temperature Co-Precipitation Synthesis of Magnetite Nanoparticles in a Large pH Window with Different

- Bases,” *Materials (Basel)*., vol. 6, no. 12, pp. 5549–5567, 2013.
- [13] Y. Zhu, Y. Liu, Y. Gao, Q. Cheng, and Z. Yang, “Magnetic properties of aristate spherical Ni nanoparticles synthesized through ultrasound reduction method,” *Mater. Res. Bull.*, vol. 87, pp. 135–139, 2017.
- [14] R. Clar, “Aplicación de nanopartículas magnéticas de hierro a la eliminación de mercurio del agua,” 2013.
- [15] K. Atacan, B. Çakiroglu, and M. Özacar, “Improvement of the stability and activity of immobilized trypsin on modified Fe₃O₄ magnetic nanoparticles for hydrolysis of bovine serum albumin and its application in the bovine milk,” *Food Chem.*, vol. 212, pp. 460–468, 2016.
- [16] W. Peternele, V. Monge Fuentes, M. L. Fascineli, J. Rodrigues Da Silva, R. Silva, C. Lucci, and R. Bentes De Azevedo, “Experimental Investigation of the Coprecipitation Method: An Approach to Obtain Magnetite and Maghemite Nanoparticles with Improved Properties,” *J. Nanomater.*, vol. 2014, no. 1, pp. 1–11, 2014.
- [17] L. Motte, “Ferrofluides - Nanoparticules superparamagnétiques,” vol. 33, no. 0, 2012.
- [18] I. Milosevic, F. Warmont, Y. Lalatonne, and L. Motte, “RSC Advances,” *RSC Adv.*, vol. 4, pp. 49086–49089, 2014.
- [19] S. Martínez, “Puesta en marcha y aplicación a polvos cerámicos del método de reflectancia difusa en espectroscopía de infrarrojo,” 2012.
- [20] J. Antonio and M. Pastor, “Análisis de óxidos de Silicio y estructuras multicapa para aplicaciones microelectrónicas,” 2000.
- [21] P. P. Supervisada, “Desarrollo de un nuevo método para medir la distribución de tiempo de residencia de Equipos.”
- [22] P. Iranmanesh, S. Saeednia, and M. Nourzpoor, “Characterization of ZnS nanoparticles synthesized by co-precipitation method,” vol. 24, no. 4, pp. 1–4, 2015.
- [23] C. Venkata, J. Shim, and M. Cho, “Synthesis , structural , optical and photocatalytic properties of CdS / ZnS core / shell nanoparticles,” *J. Phys. Chem. Solids*, vol. 103, no. December 2016, pp. 209–217, 2017.
- [24] L. Zhang, R. Dong, Z. Zhu, and S. Wang, “Sensors and Actuators B: Chemical Au nanoparticles decorated ZnS hollow spheres for highly improved gas sensor performances,” *Sensors Actuators B. Chem.*, vol. 245, pp. 112–121, 2017.
- [25] K. Wang, X. Xub, L. Ma, A. Wang, R. Wang, and J. Luo, “Studies on triboluminescence emission characteristics of various kinds of bulk ZnS crystals,” *J. Lumin.*, vol. 186, pp. 307–311, 2017.

- [26] B. Information, "Determining An Equilibrium Constant Using Spectrophotometry and Beer ' s Law," no. III, pp. 1–14.

CONFIDENTIAL

ANNEX

1. Production of Nanoparticles of Magnetite

To produce nanoparticles of Fe_3O_4 by co-precipitation methodology there are two parameters to be considered in order to obtain nanoparticles with a uniform length (between 9 and 16 nm). The methodology used is the co-precipitation. The first one is to respect concentrations of Fe^{2+} and Fe^{3+} to a proportion 1:2. The second one is to follow the molar relations explained in the table below:

Molar relations	
$\text{Fe}^{3+}/\text{Fe}^{2+}$	2
NaOH/Fe(total)	5,50
H₂O/Fe(total)	298,60
HCl/Fe²⁺	0,75

Table 1.1. Molar relations for the different reagents

The chemicals reagents used in this experiments were $\text{FeCl}_3 \cdot 6\text{H}_2\text{O}$, $\text{FeCl}_2 \cdot 4\text{H}_2\text{O}$, NaOH, distilled water and HCl. Normally when planning these experiments, it is better to fix one component and equilibrate the others with the molar relations (Fe^{2+} for example). If the Fe^{2+} is fixed to 1'5 g, then the other reagents, holding the molar relations, are as follow:

	Weight (g)	Volume (mL)	Mol
FeCl₂·4H₂O	1,5	-	0,01
FeCl₃·6H₂O	4,1	-	0,02
H₂O	-	119,5	6,64
HCl (1M)	-	5,7	0,01
NaOH (2M)	-	62	0,12

Table 1.2. Weights and volumes of reagents fixing $FeCl_2 \cdot 4H_2O$ to 1,5 grams

To prepare the solution of Fe^{3+} , we weigh the powder of $FeCl_3 \cdot 6H_2O$ to follow the relation 1:2 of Fe^{2+}/Fe^{3+} . To do so, we place it on a beaker and we add water until the relation H_2O is fulfilled. Be aware of the water contained on the Fe^{2+} and Fe^{3+} powders. Homogenize the sample with an ultrasonic-bath for 5 min.

It is better to prepare the solution of Fe^{2+} the same day the reaction is going to take place, to avoid premature oxidation. We weigh the powder of $FeCl_2 \cdot 4H_2O$, and we placed it in a beaker and we add the necessary volume of HCl to reach the relation HCl/Fe^{2+} . The HCl used for these experiments was 1 M. Homogenize the sample with an ultrasonic-bath for 5 min. Once homogenized, the solutions Fe^{3+}/Fe^{2+} should be mixed and stirred on an ultrasonic-bath to achieve the perfect molar relation Fe^{3+}/Fe^{2+} .

To prepare the solution of NaOH, we weigh the powder on a beaker and we mix it with water to obtain a 2M concentration solution. Stirred it with a magnetic agitator to homogenize.

The equipment used in the experiments was the following:

- Thermal bath
- 250 mL reactor

- Mechanical stirrer
- Peristaltic pump

The thermal bath is used to maintain the temperature of 30 °C to allow the repeatability of the experiments.



Figure 1.1. Thermal bath used

To do so, the bath is connected to the thermal shell of the reactor through plastic pipes.

A peristaltic pump is required to do the impulsion. The flow rate was set to 1,5 L/min.



Figure 1.2. Peristaltic bomb

To start the experiment, the bath was heated to 30 °C and the pump was set to 1,5 L/min. Wait 20 minutes to heat and stabilize the temperature inside the reactor. First, the NaOH solution was placed inside the reactor. Then the reactor was sealed and stirred for 1 minute.

Using another peristaltic bomb, at a speed of 400 mL/min the solution of $\text{Fe}^{2+}/\text{Fe}^{3+}$ was poured into the reactor. This procedure is relevant because the speed addition will give uniformed diameters and less agglomerations.



Figure 1.3. Reactor with thermal Shell and paddle stirrer

After adding the ferrous solution, the mix will be left for 2 hours with vigorous agitation. If the reaction is well done, the color of the solution inside will be black, indicating the magnetite is formatted.

If the nanoparticles precipitate to the bottom of the reactor when the stirring stops, it indicates agglomeration and different diameters of nanoparticles. If the size is uniform, the particles will rest in suspension. The ferrofluid is transferred to a 1 L beaker.

A specific volume of HCl 2,5 M must be added to the solution to neutralize it. This volume depends on the concentration of NaOH remaining in the solution. At this pH 7, MNP lose their surface charges and tends to aggregate themselves, becoming sensible to the magnetic field and therefor are easy to separate through magnets.

In order to do the cleanings, a magnetic separator (Figure 1.4) was used for the separation of MNP and the solution. The solution inside the beaker was first neutralized with HCl

2,5 M and then divided into 50 mL Falcon tubes. Afterwards, the tub was placed inside the magnetic separator and left for 5 min. After checking that nanoparticles have been attracted by the magnet and the solution has become transparent (like Figure 1.5), pour the solution and rinse with water. Control the pH stays at 7 and repeat the operation 4 times more.



Figure 1.4. Magnetic separator

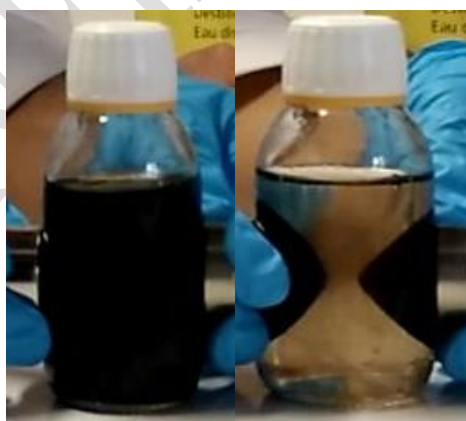


Figure 1.5. MNP separation through magnets

After washing down the samples, nanoparticles are scattered in water, adjusting the pH to 2 with a known volume of HCl. At the end, a black ferrofluid is obtained. In this state the nanoparticles are stable.

The concentration of Fe_3O_4 nanoparticles is done by spectroscopy UV. The equation used in this case is as follows:

$$[Fe] = \frac{Abs_{480} \times k}{\varepsilon \times L} = \frac{Abs_{480} \times 300}{420 \times 1} \quad (1)$$

The UV is done at a wave length $\lambda=480$ nm, being Abs (absorbance) given by the UV spectroscopy, k (factor of dilution), ε (absorptivity) and L (length of the optical path containing the sample). In this case for Fe_3O_4 nanoparticles k oscillates between 300 and 500 depending on the volume used to wash the nanoparticles. ε equals to 420 l/mol·cm and L 1cm. To calculate the concentration of Fe_3O_4 do the conversion as it follows:

$$[Fe] \frac{mol}{l} \times \frac{1 mol Fe_3O_4}{3 mol Fe} \times \frac{231.53 g Fe_3O_4}{1 mol Fe_3O_4} = [Fe_3O_4] \frac{g}{l} \quad (2)$$

2. Functionalization of SiC with magnetic nanoparticles

In this work, the method used implied a direct mixing between SiC and nanoparticles. It was chosen due to its simplicity (lack of organic solvents and expensive equipment) and reproducibility. Four types of experiments were made in order to functionalize the SiC:

1. Synthesis of MNP with SiC simultaneously
2. Addition of MNP already produced with mechanical agitation
3. Water evaporation
4. Use of a binder

All experiments were realized with a 10% of mass concentration between SiC and Fe_3O_4 nanoparticles.

$$\frac{g Fe_3O_4}{g SiC} \times 100 = 10\% \quad (3)$$

4.1. Synthesis of magnetic nanoparticles with SiC simultaneously

The process is realized with the same reactor used earlier in the production of MNP. We prepare the solutions of Fe^{3+} , Fe^{2+} and NaOH with the same concentrations as in the previous chapter. Place the NaOH and the SiC particles in the reactor and add the ferrous solution with vigorous agitation. Stir for 2 hours to form the nanoparticles and maximize the interactions between SiC and Fe_3O_4 .

To separate the nanoparticles that haven't coated the SiC, it is important to filtrate the sample. To do it, we use a Büchner funnel, a Büchner flask and a void pump to filtrate the solution. A filter of 8 μm was placed inside the Büchner funnel to retain the SiC particles (with a diameter 75 μm) allowing the nanoparticles to pass through it (medium size between 9 nm and 15 nm). The Büchner can be seen in the next Figure 2.1.

Magnetic SiC was rinsed with water three or four times in order to remove residual nanoparticles. The filter was placed in an oven to dry the particles.

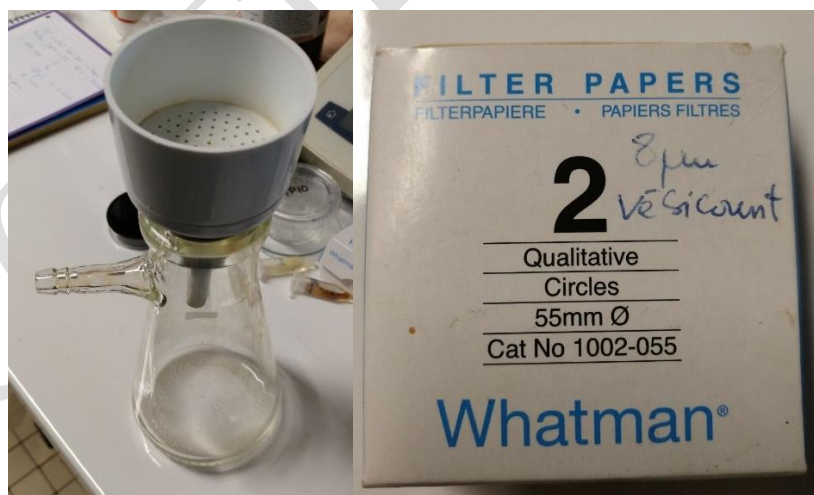


Figure 2.1. Büchner funnel and Büchner flask and paper filter

4.2. Addition of magnetic nanoparticles already produced with mechanical agitation.

This technique uses the same equipment as the section 4.1 Synthesis of magnetic nanoparticles with SiC simultaneously. In this case, the nanoparticles were already manufactured. The nanoparticles are stable at a $\text{pH} = 2$ and the reaction must take place at a $\text{pH} = 12$. To set the pH of the reaction and avoid premature precipitation of nanoparticles, the SiC is placed at the bottom of the reactor with 20 mL of NaOH 2M. Once the mixing SiC-NaOH is well stirred, we add the nanoparticles and agitate them for 2 hours.

The separation process between nanoparticles and magnetic SiC follows the same parameters as section 4.1 Synthesis of magnetic nanoparticles with SiC simultaneously.

4.3. Water evaporation

On the first assumption, solvent could hinder the coating of SiC at the end of the reaction, the water evaporation was tested to evaluate the initial assumption. The equipment used in this case was a Rotavapor R-100 (Buchi®), integrating a condenser, void pump, thermal bath and a mechanical rotation. The rotavapor used is showed in the following Figure 2.2. Rotavapor R-100. Figure 2.2



Figure 2.2. Rotavapor R-100.

In the evaporation flask, the weight of SiC was placed with 20 mL of NaOH. Then, the nanoparticles were added and the evaporation flask was connected to rotavapor. Setting the temperature to 50 °C and a pressure of 75 mbar, the volume was agitated through rotation.

This process takes approximately 30 minutes to evaporate all the solvent. To remove the content from the Erlenmeyer, add 200 mL of water and stir the content. Then, with the same method as section 4.1 Synthesis of magnetic nanoparticles with SiC simultaneously, separate the magnetic SiC from the nanoparticles solution by filtration process.

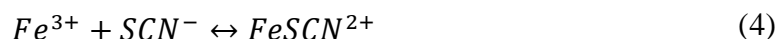
4.4. Use of a binder

In this technique, hydroxypropyl methylcellulose (HPMC) was added to the mixing of SiC and nanoparticles. The binder is used with proportions between 0,5 and 1% of the total weight of SiC. To dissolve the HPMC, we place the powder inside a flask of 10 mL and add 5 mL of water. Afterwards, we place the flask on a magnetic agitator and set the plate to 40°C. Once dissolved, allow the solution to cool at room temperature.

The binder can be used in the mechanical addition or the water evaporation. On both cases, the binder should be the last solution to be mixed.

3. Concentration determination by the method KSCN

To know the exact concentration of nanoparticles, a full oxidation is required. The nanoparticles created of Fe₃O₄ are a mixture of Fe²⁺ and Fe³⁺. In order to form the complex FeSCN²⁺, and to obtain a solution which has its band of absorbance at 475nm, all Fe²⁺ must be transformed in Fe³⁺ [26].



First, the concentration of the nanoparticles solution must be between 2 mM and 20 mM of Fe, which are the detection limits. To do so, we calculate the theoretical concentration of Fe and we dilute it till 15 mM are reached. For example, with 1.5 g of $\text{FeCl}_2 \cdot 4\text{H}_2\text{O}$ and 4,5 g of $\text{FeCl}_3 \cdot 6\text{H}_2\text{O}$ and a volume of 187,6 mL the theoretical concentration of Fe is 0.12 M.

$$1.5 \text{ g FeCl}_2 \cdot 4\text{H}_2\text{O} \times \frac{1 \text{ mol FeCl}_2 \cdot 4\text{H}_2\text{O}}{198.83 \text{ g FeCl}_2 \cdot 4\text{H}_2\text{O}} \times \frac{1 \text{ mol Fe}}{1 \text{ mol FeCl}_2 \cdot 4\text{H}_2\text{O}} = 0.0075 \text{ mol Fe} \quad (5)$$

$$4.5 \text{ g FeCl}_3 \cdot 6\text{H}_2\text{O} \times \frac{1 \text{ mol FeCl}_3 \cdot 6\text{H}_2\text{O}}{270.35 \text{ g FeCl}_3 \cdot 6\text{H}_2\text{O}} \times \frac{1 \text{ mol Fe}}{1 \text{ mol FeCl}_3 \cdot 6\text{H}_2\text{O}} = 0.015 \text{ mol Fe} \quad (6)$$

$$\frac{\text{mol Fe}}{\text{Total Volume}} = \frac{0.0075 \text{ mol Fe} + 0.015 \text{ mol Fe}}{0.1876 \text{ L}} = 0.12 \text{ mol/L Fe} \quad (7)$$

To place it to 15 mM, dilute 84 μL of nanoparticles solution in 1 mL of deionized water with a factor 12 dilution.

Once the solution is ready in a Falcon tube of 15 mL, place the next reagents:

1. 10 μL of nanoparticles solution 15 mM [fe]
2. 100 μL of a H_2O_2 solution 20% m/m
3. 100 μL of a HNO_3 solution 7 M

Heat the falcon tube in a thermal bath for 2-3 hours to destroy the nanoparticles and oxidize Fe^{2+} to Fe^{3+} .

4. Add 1 mL of deionized water
5. 100 μL of a KSCN solution 2M

Once the KSCN is introduced inside the falcon tube it is important to measure the absorbance immediately. Place the UV to 475 nm and measure the absorbance. The blanc used was water. With the following equation, the concentration of Fe can be found:

$$Abs_{475\text{ nm}} = 0.054 \times [Fe]_{on\text{ mM}} \times Dilution\ factor \quad (8)$$

For a direct measure of nanoparticles concentration, the wave length was 480 nm ($\lambda=480$ nm), the dilution factor was 1/300, ϵ was 420 and L being 1 cm. With the following equation, the concentration was determined:

$$[Fe] = \frac{Abs_{480\text{ nm}} \times Dilution\ factor}{\epsilon \times L} \quad (9)$$

CONFIDENTIAL